Progress In Electromagnetics Research M, Vol. 96, 169–179, 2020

Application of Stub-Loaded Step-Impedance Resonator for Quint-Band Bandpass Filter Design

Li-Qin Liu[1], Min-Hang Weng[1], Ya-Bin Weng[1], Chin-Yi Tsai[2], and Ru-Yuan Yang[2, *]

Abstract—Stub-loaded step-impedance resonator (SLSIR) is a multi-mode resonator and can be applied to implement multi-band or wideband filters. In this paper, odd- and even mode impedance analysis is used to resonant properties of the SLSIR. Only two SLSIRs are applied to design a quint-band bandpass filter (BPF). To find the required five resonant modes, the frequency ratios of the high order modes to the fundamental mode of the SLSIR are calculated depending on the impedance ratio and the length ratio of the SLSIR. Several coupling types of the SLSIRs are considered first to have enough energy for all the five passbands. When forming the quint-band, a pair of the SLSIR are coupled electrically and connected with a 0° feeding input/output structure. The center frequencies are designed at 1.38 GHz, 2.58 GHz, 3.69 GHz, 5.36 GHz, and 5.8 GHz, corresponding to the different communication applications. The filter is designed, fabricated, and measured. Simulated and experimental results are in agreement, verifying the design concept.

1. INTRODUCTION

Recently, multi-service mobile wireless communication systems are more and more popular for commercial products. Bandpass filter (BPF) in RF front end is a key component and shall provide two or more frequency bands, thus multi-band BPFs have been developed aggressively to achieve the newly developed multi-service system and the commercial products. Microstrip resonator is a planar structure and easy to be integrated with other active circuits and then is suitable for the filter design. Figure 1 shows various communication systems and corresponding frequencies. For example, navigation satellite timing and ranging global position system (GPS) uses frequency bands of 1.22 GHz, 1.38 GHz, and 1.575 GHz; China mobile system in the 4th Generation (4G) uses frequency band of $2.575 \sim 2.635$ GHz; wireless local area network (WLAN) system uses frequency bands of 2.4 GHz and $5.15 \sim 5.8$ GHz; and worldwide interoperability for microwave access (WIMAX) system uses frequency band of $3.3 \sim 3.8$ GHz.

In past, many researchers have developed microstrip multi-pass band filters using multi-mode resonator (MMR). In various types of the MMR, step-impedance resonator (SIR) and stub-loaded resonator (SLR) are very popular for the design of multi-band BPF since there are many resonant modes to be controlled to the desired frequency [1–4]. For example, in Hsu et al.'s work, a second-order tri-band BPF designed using a three-stage stub-loaded SIR (SLSIR) was introduced, and cross-coupling was used to sharpen the passband skirt [5]. In Chen and Chu's work, a four-band BPF with independently controllable center frequency was obtained using SIR combined with a shaft-mounted resonator [6].

In Hsu et al.'s work, a double-layer structure with greater design flexibility was used to provide multipath for different frequency bands to implement a quint-band BPF [7]. In Chen's work, a three-mode SIR with branches was used to achieve a quint-band BPF, but it has a large insertion loss [8]. In Chen and Wei's work, a five-mode SLR was proposed to implement a quint-band BPF by controlling

Received 29 June 2020, Accepted 4 September 2020, Scheduled 24 September 2020
* Corresponding author: Ru-Yuan Yang (ryyang@mail.npust.edu.tw).
[1] School of Information Engineering, Putian University, Putian, Fujian 351100, China. [2] Graduate Institute of Materials Engineering, National Pingtung University of Science and Technology, Pingtung County 912, Taiwan.

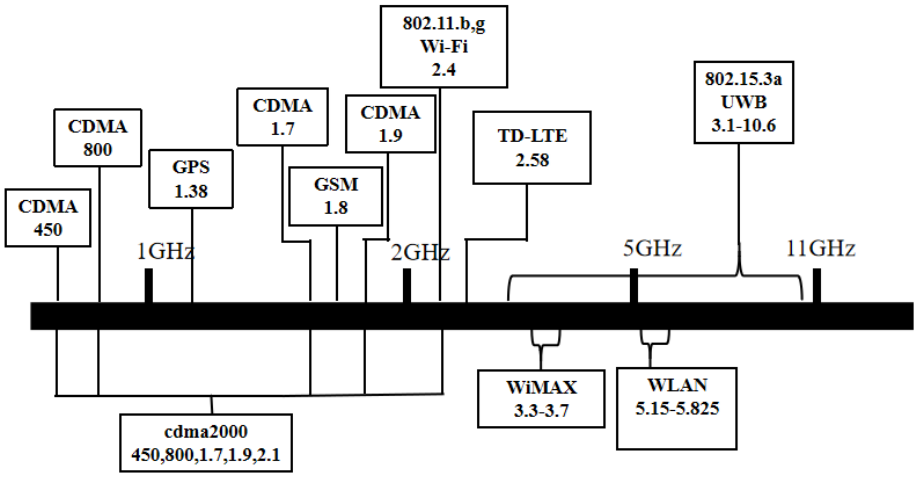

Figure 1. Various communication systems.

the impedance and length of the SLR [9]. In Xu et al.'s work, a multi-stub-loaded ring resonator was used to design a quint-band BPF with electromagnetic coupling [10]. In Zhu et al.'s work, two penta-mode resonators (PMRs) were used to implement a quint-band BPF [11]. The PMR can independently control the first five resonant modes by shorted high-impedance section of quarter-wave SIRs and four loaded open stubs. In Ai et al.'s work, a quint-band BPF with mixed electric and magnetic coupling (MEMC) was implemented based on an MMR and a $\lambda/4$ resonator [12]. In Zhou et al.'s work, tri-/quad-/quint-/sext-band BPFs with flexible frequency and bandwidth allocations are presented by incorporating substrate-integrated waveguide (SIW) dual-mode resonances with split-type dual- and triple-band symmetrical frequency responses [13].

In a previous work, SLSIR was used to design a tri-band BPF [3]. However, the previous research was designed based on the analysis results of only a few design parameters [3] and did not analyze the higher-order modes of SLSIR under different design parameters. Therefore, it is difficult to find suitable design parameters to achieve the required five passbands. Moreover, the quint-band filter designed in the past literature usually used several resonators. Thus, it is still a challenge to design a quint-band filter with only two resonators. The contribution of this study is to further analyze various high-order modes of an SLSIR structure with various possible design parameters, and then only using two SLSIRs is applied to design a compact quint-band filter.

In this paper, the resonant properties of an SLSIR is further analyzed first depending on the impedance ratio and the length ratio of the SLSIR. Different coupling types are considered to have enough energy for all the five passbands. For forming the quint-band, two pairs of the SLSIR are arranged face to face with electrical coupling to have enough coupling energy. Input/output (I/O) ports are connected to the SLSIRs with a 0° feeding structure. The center frequencies are designed at 1.38 GHz, 2.58 GHz, 3.69 GHz, 5.36 GHz, and 5.8 GHz, corresponding to the GPS, 4G, WIMAX, and WLAN applications, respectively. Moreover, transmission zeros near passband edge of each passband are obtained due to use of the 0° feeding structure, thus improving the band selectivity.

2. DESIGN PROCEDURE

2.1. Odd and Even Mode Analysis of Resonances of SLSIR

Figure 2 shows the configuration of the SLSIR, which mainly composes a typical SIR with a stub loaded at the symmetric line (S-S') of the SIR. The impedance and electrical length of two different sections of the SIR are expressed as (Z_1 and θ_1) and (Z_2 and θ_2), and the stub has the impedance Z_s and electrical length θ_s. The analysis of resonant behavior of the SLSIR is required to understand the frequency of various resonant modes. Thus, two impedance ratios K_1, K_2 can be defined and expressed as $K_1 = Z_2/Z_1$ and $K_2 = Z_s/Z_1$, respectively. The input admittance Y_{in} of the SLSIR can be derived,

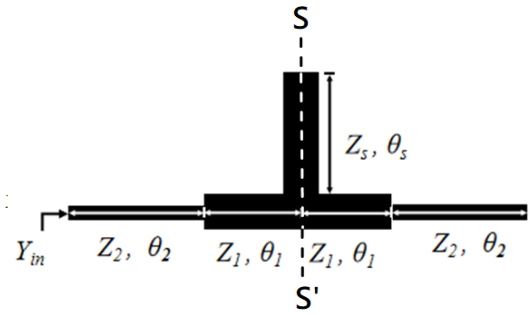

Figure 2. The schematic of the SLSIR.

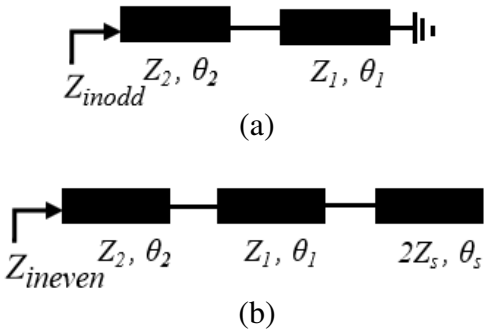

Figure 3. The layout of the SLSIR under (a) odd-mode resonance and (b) even-mode resonance.

and when setting the condition of the input admittance $Y_{in} = 0$, the solutions satisfying the condition are the resonant modes of the SLSIR.

However, since the used SLSIR is symmetric, the odd and even impedance analysis for analyzing the resonant properties is more popular. In the odd-mode resonance, the symmetry plane of the SLSIR is an electric wall, and in the eve-mode resonance, the symmetry plane of the SLSIR is a magnetic wall. Figure 3 shows the layout of the SLSIR under (a) odd-mode resonance and (b) even-mode resonance. Also based on the transmission theory [14], the resonant condition corresponding to the odd- and even-mode resonances of the SLSIR can be expressed as Eqs. (1a) and (1b), respectively:

$$(K_1 - \tan\theta_1 \tan\theta_2) = 0 \tag{1a}$$

$$[2K_2 (K_1 \tan\theta_1 + \tan\theta_2) + \tan\theta_s (K_1 - \tan\theta_1 \tan\theta_2)] = 0 \tag{1b}$$

Since there are three electrical lengths θ_1, θ_2, and θ_s, two other length ratios can be defined to obtain more design freedom. The length ratio (α) of the SIR with two discontinuities and the length ratio (r) of the stub are also varied to adjust the higher order resonant modes over a wide frequency range. The first length ratio (α) is defined as $\alpha = 2\theta_2/2(\theta_1 + \theta_2) = 2\theta_2/\theta_T$, and the second length ratio (r) is $r = 2\theta_S/\theta_T$, where θ_T is the total length of the SIR section. K_1, K_2 are defined as the impedance ratios expressed as $K_1 = Z_2/Z_1$ and $K_2 = Z_s/Z_1$, respectively.

In order to plot the resonant curves for various different parameters K_2, α and r, Z_s is set equal to Z_1, i.e., $K_2 = 1$, thus also simplifying the design. After substituting formulas of length ratio (α) and the length ratio (r) into Eqs. (3a) and (3b), the resonant condition corresponding to the odd- and even-mode resonances as a function of α, r, and K_1 can be obtained as Eqs. (2a) and (2b).

$$K_1 - \tan\left(\frac{1-\alpha}{2}\theta_T\right)\tan\left(\frac{\alpha}{2}\theta_T\right) = 0 \tag{2a}$$

$$2\left(K_1 \tan\left(\frac{1-\alpha}{2}\theta_T\right) + \tan\left(\frac{\alpha}{2}\theta_T\right)\right) + \tan\left(\frac{r}{2}\theta_T\right)\left(K_1 - \tan\left(\frac{1-\alpha}{2}\theta_T\right)\tan\left(\frac{\alpha}{2}\theta_T\right)\right) = 0 \tag{2b}$$

Therefore, the solutions of Eqs. (2a) and (2b) are related to the odd and even resonant modes dependent on α, r, and K_1. Figure 4 shows calculated ratios of the higher resonant frequencies to the fundamental resonant frequency for the SLSIR using MATLAB tool at various length ratios $r = 0.1$, 0.3, 0.5, 0.7, and 0.9 based on (a) $K_1 = 4$ and $K_2 = 1$, (b) $K_1 = 2$ and $K_2 = 1$, (c) $K_1 = 0.5$ and $K_2 = 1$, (d) $K_1 = 0.25$ and $K_2 = 1$. The fundamental resonant frequency (f_1), the third resonant frequency (f_3), and the fifth resonant frequency (f_5) also result from the odd mode resonance of the SLSIR. In addition, the second resonant frequency (f_2) and the forth resonant frequency (f_4) result from the even mode resonance of the SLSIR. It is noted that many sets of the impedance ratios K_1 and K_2 can be used in the design of the quint-band BPF.

When selecting the resonant modes for the passbands meeting the requirement of GPS of 1.38 GHz, 4G of 2.58 GHz, WiMAX of 3.69 GHz, and WLAN of 5.36/5.8 GHz, $f_2/f_1 = 2.58/1.381.87$, $f_3/f_1 = 3.69/1.382.67$, $f_4/f_1 = 5.36/1.383.88$, and $f_5/f_1 = 5.8/1.384.2$ are calculated first and mapped to

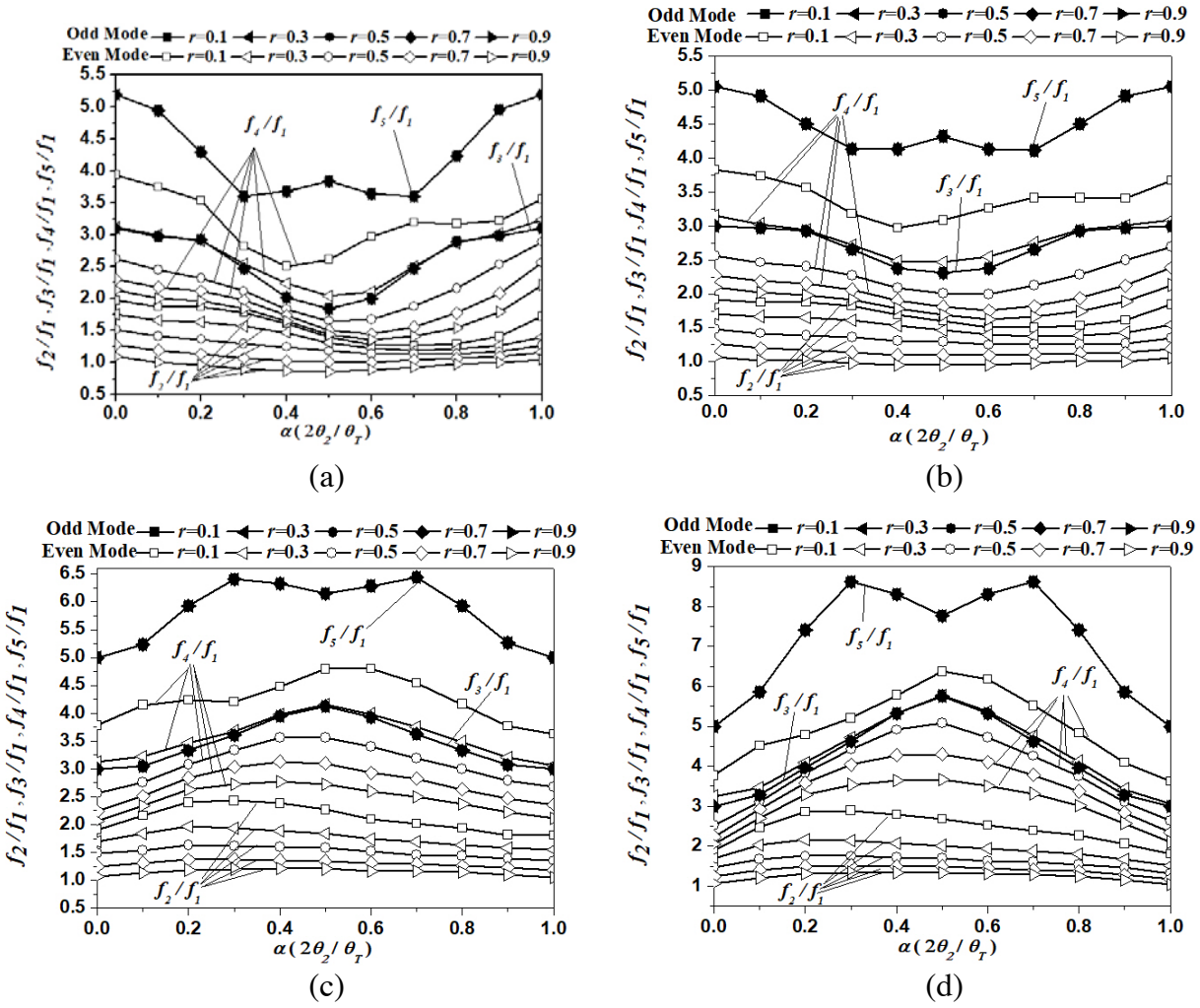

Figure 4. Calculated ratios of the higher resonant frequencies to the fundamental resonant frequency for the SLSIR using MATLAB tool at various length ratio $r = 0.1$, 0.3, 0.5, 0.7 and 0.9 based on (a) $K_1 = 4$ and $K_2 = 1$, (b) $K_1 = 2$ and $K_2 = 1$, (c) $K_1 = 0.5$ and $K_2 = 1$, (d) $K_1 = 0.25$ and $K_2 = 1$.

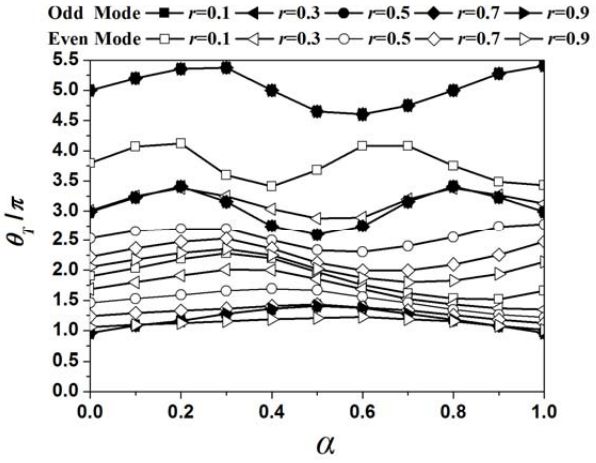

Figure 5. Calculated length ratio α with resonant electric length θ_T for the SLSIR using MATLAB tool at various length ratio $r = 0.1$, 0.3, 0.5, 0.7 and 0.9 based on $K_1 = 4$ and $K_2 = 1$.

Figure 4. $K_1 = 4$ and $K_2 = 1$ are first selected; the length ratio α is overtly selected as 0.2; and r is overtly selected as 0.1 to be the initial structure parameters of the SLSIR.

Figure 5 shows the calculated length ratio α with resonant electric length θ_T for the SLSIR using MATLAB tool at various length ratios $r = 0.1$, 0.3, 0.5, 0.7, and 0.9 based on $K_1 = 4$ and $K_2 = 1$. With mapping α as 0.2 and r as 0.1 of Figure 5, the electrical lengths θ_1, θ_2, and θ_S are obtained as 86.4°, 21.6°, and 10.8°, respectively. To obtain the physical structure, the high impedance Z_2 is fixed as 140 Ω, and the low impedance Z_1 of the SIR section and Z_S of the stub are then fixed as 35 Ω. To meet α of 0.2 and r of 0.1, other physical sizes of the SLSIR and stub are: $L_1 = 17.6$ mm, $L_2 = 45$ mm, $L_3 = 5.9$ mm, $L_4 = 12.9$ mm, $W_1 = W_2 = 4$ mm, and $W_3 = 0.3$ mm.

2.2. Design of Quint-Band Filter

The quint-band BPF is expected by combining two SLSIRs selected above with input/output (I/O) ports. The specifications of the designed BPF are centered at 1.38 GHz, 2.58 GHz, 3.69 GHz, 5.36 GHz, and 5.8 GHz, with 3-dB fractional bandwidths (FBW) of 10%, 8%, 4.6%, 5%, and 2.5%, respectively. Therefore, the element values for the low-pass Chebyshev prototype with 2 dB ripple are found to be $g_0 = g_2 = 1$, $g_1 = 1.5296$, where g_n for $n = 0$ to 2 is the element value. The BPF is designed and fabricated on a 0.787 mm thick RT/Duroid 5880 substrate, having a dielectric constant of $\varepsilon_r = 2.2$ and loss tangent of 0.0009. A full-wave electromagnetic (EM) simulator is used for this simulation work [15]. There are several types of resonator arrangement for the filter design such as electric coupling, magnetic coupling, and mixed coupling [14]. To provide the desired coupling energy, two SLSIRs are arranged face to face to have electric coupling. With considering the connected position of the I/O ports, different types are considered first to have enough energy for all the five passbands.

Figure 6 shows simulated filter responses of the designed quint-band BPF with different connected positions, comprising (a) electrical coupling and direct connection, (b) electrical coupling and 0° feeding structure, (c) magnetic coupling and a direct connection, (d) magnetic coupling and 0° feeding structure,

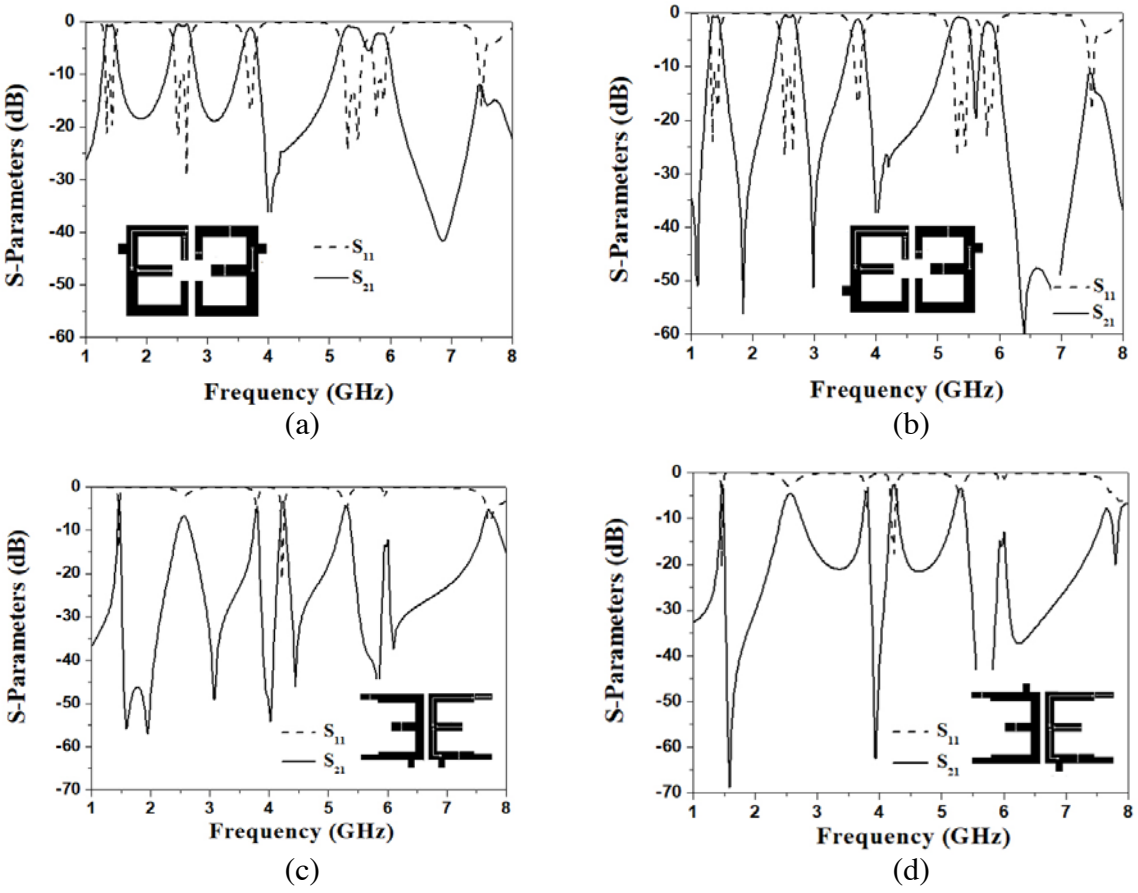

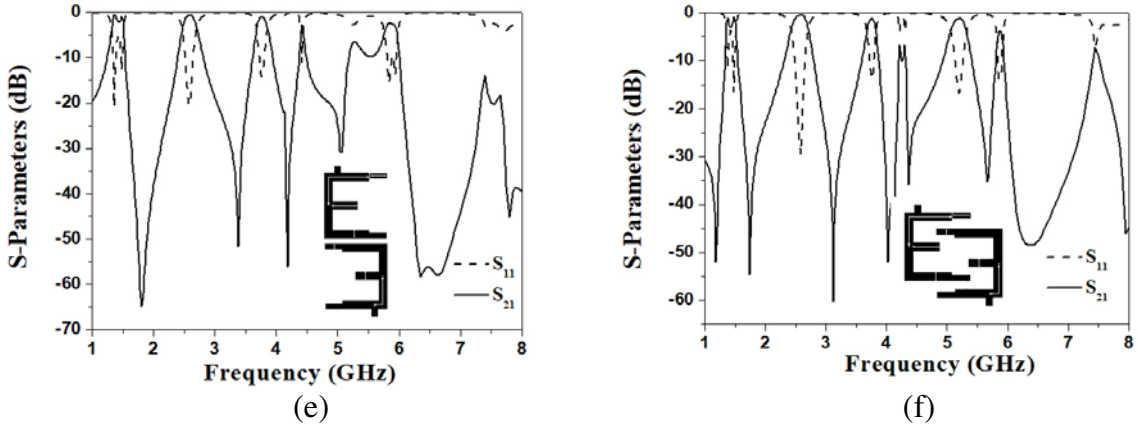

Figure 6. Simulated filter responses of the designed quint-band BPF with (a) electrical coupling and a direct connection, (b) electrical coupling and 0° feeding structure, (c) magnetic coupling and a direct connection, (d) magnetic coupling and 0° feeding structure, (e) mixed coupling and a direct connection, (f) interdigital coupling and 0° feeding structure.

(e) mixed coupling and a direct connection, (f) interdigital coupling and 0° feeding structure. When the filter performances are simulated, the structure parameters of these different filters are all similar except the connected position (t), and these filters are not yet optimum. It is clearly found that electrical coupling for two SLSIRs is much easier to obtain the quint-band response. Since the presented topology corresponds to an all-pole configuration where two multi-mode resonators are coupled, the way to generate transmission zeros in the all-pole configuration might typically result from a direct source-to-load coupling. In the two electrical coupling schemes as shown in Figures 6(a) and 6(b), it is found that even in the all-pole configuration, direct connection of the I/O ports does not provide the transmission zeros between the passbands or near the passband edges; however, the transmission zeros are clearly observed between the passbands or near the passband edges when the 0° feeding structure of the I/O ports [16] is used. Thus, two SLSIRs with electrical coupling and the 0° feeding structure of the I/O ports, as the type of Figure 6(b), are used in this design.

Based on the known structure parameters of the SLSIR, the resident two parameters of the designed BPF are the coupling gap (g) and connected position (t). Figure 7 shows the configuration of the proposed quint-band BPF. To determine the coupling gap (g), the coupled filter theory is used when the filter has coupling type. The theoretical coupling coefficients $M_{i,j}$ can be calculated first to satisfy the filter specification for the bandwidths of each passbands, as expressed as [14]:

$$M_{i,j} = \frac{\text{FBW}}{\sqrt{g_1 g_2}} \tag{3}$$

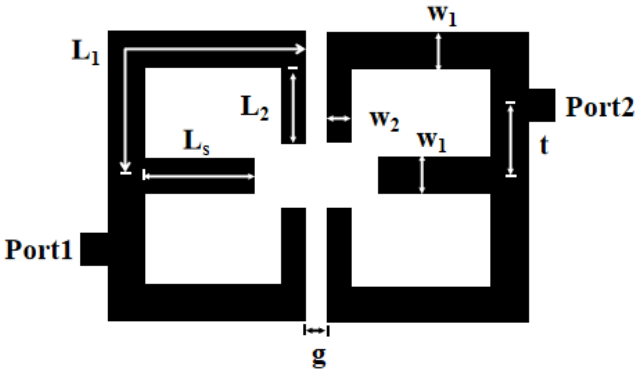

Figure 7. Schematic of the proposed quintuple-band BPF.

where FBW is the 3 dB fractional bandwidth, and g_n and g_{n+1} are element values of the filter response function. Based on the element values, the coupling coefficients $M_{i,j}$ are calculated as 0.096, 0.08, 0.032, 0.045, and 0.024 for five band frequencies, respectively. The calculated coupling coefficients ($K_{i,j}$) are calculated from full-wave simulated response under weak coupling, expressed as [14]:

$$K_{i,j} = \frac{f_H^2 - f_L^2}{f_H^2 + f_L^2} \tag{4}$$

where f_H and f_L are the higher and lower resonant frequencies of the two split resonant modes at resonance.

Figure 8 shows the calculated coupling coefficient ($K_{i,j}$) of five passbands. The coupling spacing (g) is then roughly selected as 0.2 mm to meet the desired coupling coefficients. When the connected position (t) of the I/O ports is dealt with, the 0° feeding structure is also used since the arrangement typically results in a pair of transmission zeros near each passband edge, according to the theoretical analysis reported in [16], which provides high isolation and selectivity of the passband.

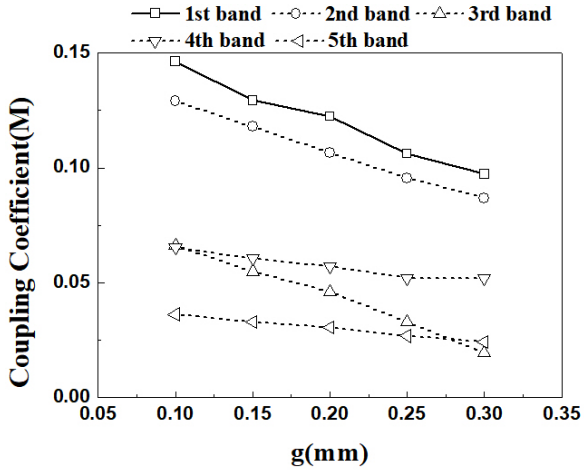

Figure 8. The coupling coefficient of the five passbands.

The connected position (t) is determined from the external quality, Q_e. The theoretical external quality Q_{en} can be calculated first to satisfy the filter specification for the bandwidths of each passband, as expressed as [14]:

$$Q_{en} = \frac{g_0 g_1}{\text{FBW}} \tag{5}$$

where FBW is the 3 dB fractional bandwidth, and g_n and g_{n+1} are element values of the filter response function. Also based on the element values, the theoretical external quality Q_{en} is 13, 16, 34, 26, and 50 for five band frequencies. The practical external quality (Q_e) can be calculated from the simulated filter response, expressed as:

$$Q_e = \frac{2\omega_0}{\Delta\omega_{3\,\text{dB}}} \tag{6}$$

where ω_0 is the resonant frequency, and $\Delta\omega_{3\,\text{dB}}$ is the 3 dB bandwidth of S_{21} at resonance. It is found that the theoretical external quality Q_{en} of the first four band frequencies is much lower than that of the fifth band frequency. Moreover, the suitable external quality (Q_e) for five band frequencies does not seem to be near the same connected position (t). Therefore, the theoretical external quality Q_{en} of the fifth band frequency is adopted to determine the required connected position, and then calculate the external quality (Q_e) of the first four band frequencies at the required connected position. Figure 9 shows the calculated external quality factors (Q_e) of the 5th passband with respect to the connected position of t. When mapping into Figure 7, t is roughly chosen to be 8 mm, and Q_e is 55 at 5.8 GHz. The calculated the external quality (Q_e) of the first four band frequencies at the required connected position (t) of 8 mm are 6, 8, 12, and 10.

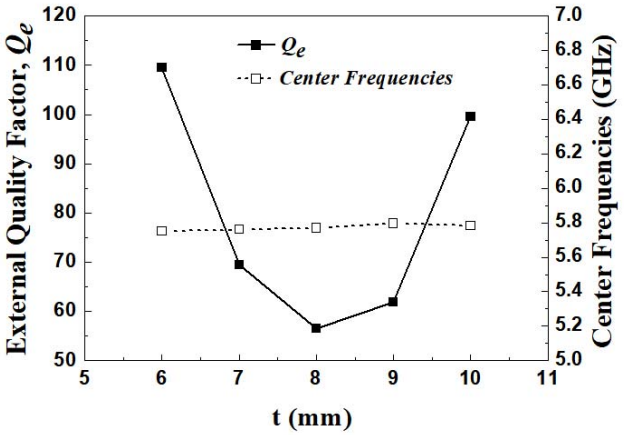

Figure 9. The external quality factors of the 5th passband respect to connected position of t.

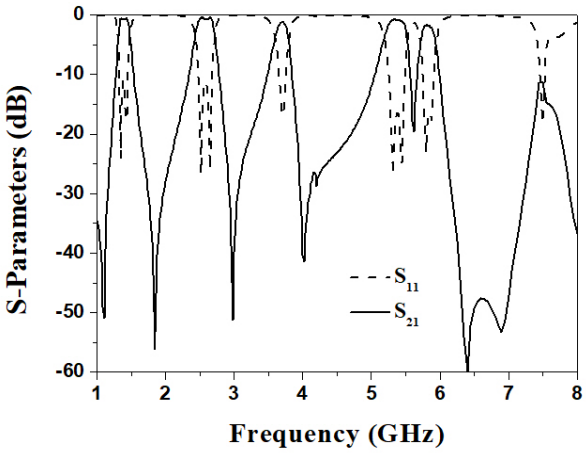

Figure 10. Simulated filter responses of the designed quint-band BPF having $L_1 = 36.1\,\text{mm}$, $L_2 = 12.9\,\text{mm}$, $Ls = 5.9\,\text{mm}$, $W_1 = 4\,\text{mm}$, $W_2 = 0.3\,\text{mm}$, $t = 9.8\,\text{mm}$ and $g = 0.2\,\text{mm}$.

After obtaining all the structure parameters of the designed filter, the filter performance can be further simulated and optimized by slightly tuning the structure parameters. Figure 10 shows simulated filter responses of the designed quint-band BPF having $L_1 = 36.1\,\text{mm}$, $L_2 = 12.9\,\text{mm}$, $Ls = 5.9\,\text{mm}$, $W_1 = 4\,\text{mm}$, $W_2 = 0.3\,\text{mm}$, $t = 9.8\,\text{mm}$, and $g = 0.2$. It is clearly observed that five passbands are formed with transmission zeros appearing near each passband, much improving the band selectivity. To find the fabrication tolerance, Figure 11 further shows simulated filter responses of the designed quint-band BPF with $g = 0.15\,\text{mm}$, $0.2\,\text{mm}$, and $0.25\,\text{mm}$. (a) first band, (b) second band, (c) third band, and (d) fourth and fifth bands. Although the gap $g = 0.15\,\text{mm}$ would better filter performances including low insertion losses and high return losses, it is difficult to be fabricated by the curve-machine. Thus, gap $g = 0.2\,\text{mm}$ is used in the fabricated filter sample.

In summary, the procedure of designing a multiband filter with different passband frequencies and bandwidths based on the proposed method is summarized as follows:

1. Analyze the high-order resonant modes under various design parameters of the SLSIR in a wide range;

2. Arrange the desired input/output ports for the resonators;

3. Determine the desired value of the coupling gap (g) by matching the theoretical coupling coefficients $M_{i,j}$ and calculated coupling coefficients $K_{i,j}$;

4. Determine the desired value of the connected position (t) by matching the theoretical external

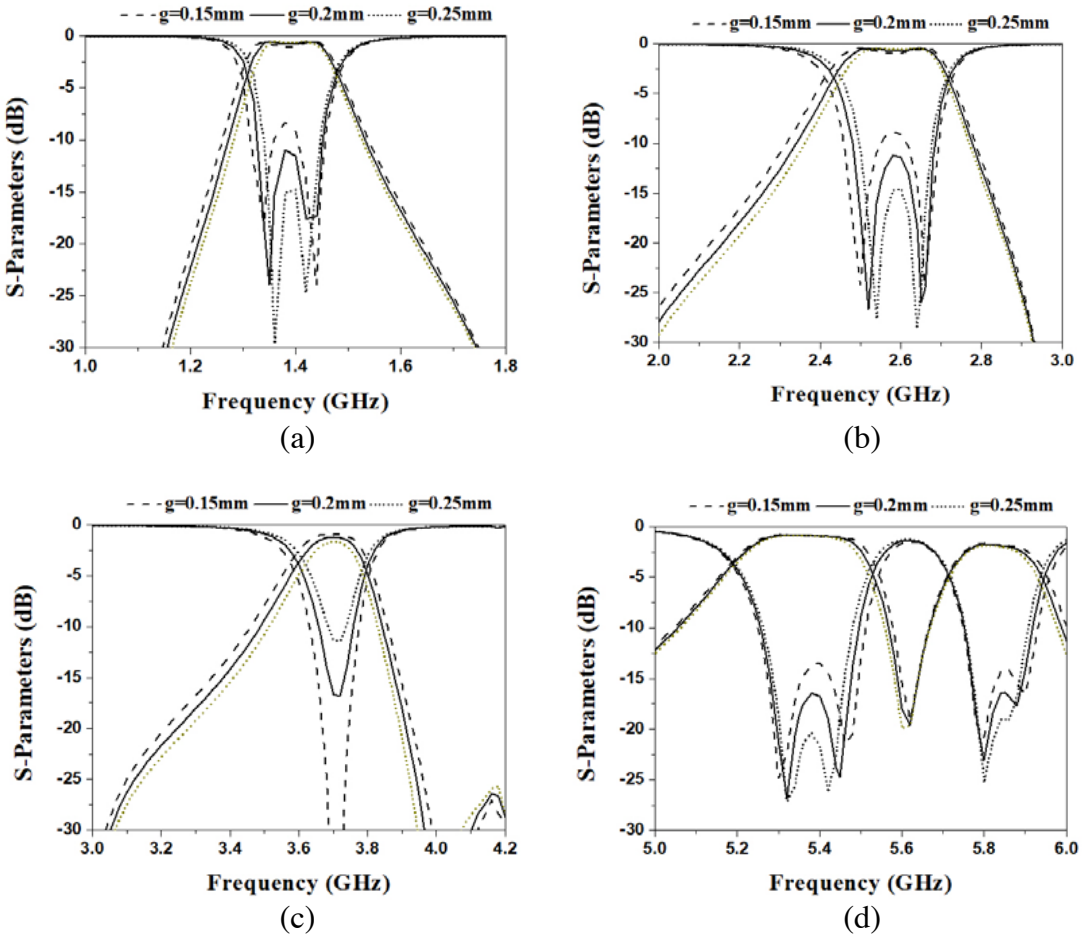

Figure 11. Simulated filter responses of the designed quint-band BPF with $g = 0.15$ mm, 0.2 mm and 0.25 mm, (a) first band, (b) second band, (c) third band and (d) fourth and fifth bands.

quality, Q_{en}, and and calculated external quality, Q_e;

5. Optimize the passband performances by slightly tuning the structure parameters.

3. FABRICATION AND MEASUREMENTS

The final dimensions for the designed BPF after an optimal design process with slightly tuning the initial values of the filter structure parameters are chosen as follows: $L_1 = 36.1$ mm, $L_2 = 12.9$ mm, $Ls = 5.9$ mm, $W_1 = 4$ mm, $W_2 = 0.3$ mm, $g = 0.2$ mm, and $t = 9.8$ mm. At the frequency of 1 GHz and 6.0 GHz, the strip widths of 2.4 mm have characteristic impedance of 49.98 and 50.04 Ω, respectively. Namely, the I/O ports with strip widths of 2.4 mm have the wide impedance match of 50 Ω in the operating bands from 1 to 6 GHz, thus reducing the return loss due to the impedance mismatch. The filter is measured by the network analyzer after the calibration procedure. Figure 12 shows the simulated and measured results for the designed quint-band BPF. The picture of the fabricated sample is inserted in Figure 12. The whole size of the quintuple-band filter is 49.7 mm × 56.9 mm, i.e., approximately $0.29\lambda_0$ by $0.34\lambda_0$, where λ_0 is the free-space wavelength at the center frequency of the first passband. The filter can be further miniaturized by folding the structure. Measured results have average insertion losses of 0.56/0.53/1.20/0.86/1.9 dB, average return losses of 10/12/14/16/9 dB, and 3-dB FBW of 12.4/10.7/4.61/5.71/3.05, for the passbands at 1.38 GHz, 2.58 GHz, 3.69 GHz, 5.36 GHz, and 5.8 GHz, respectively. Several transmission zeros which result from the 0° feeding structure of the connected I/O ports are located at 1.2, 1.8, 3.2, 4.3, and 5.6 GHz, improving the band selectivity and the isolation

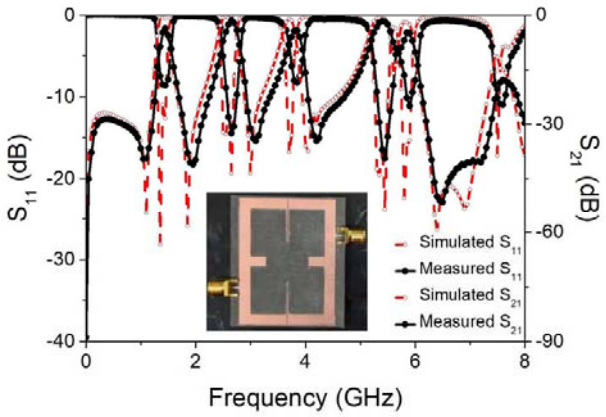

Figure 12. The simulated and measured results for the proposed quintuple-band BPF (insert plot is the photograph of the fabricated BPF).

between two passbands. Although a slight mismatch is observed at the fifth passband which might result from the fabrication error due to the thick carving knife and can be expected to be improved by precious fabrication technology. These measured results still show an agreement with the simulated ones, verifying the design concept.

Table 1 illustrates the comparisons of the designed filter with other published quint-band BPFs [10–13]. The designed BPF holds acceptable performances such as insertion loss and five transmission zeros. Moreover, the most important feature of the designed filter is its simple filter structure, as well as the miniaturized size. The insertion loss and circuit size can be further reduced by implementing low loss ceramic in the future. It is verified that by carefully choosing the impedance ratio and length ratio, SLSIR can be used to design the filter with not only three passbands [3] but also five passbands.

Table 1. Comparisons of this work with other published quint-band filters.

	f_n (GHz)	$\|S_{21}\|$ (dB)	3 dB-FBW (%)	circuit size ($\lambda_0 \times \lambda_0$)
Ref. [10]	0.63/1.33/2.03/2.74/3.45	0.47/1.14/1.8/2.2/2.5	28.8/9.4/2.7/5.3/5.5	0.043×0.178
Ref. [11]	0.63/1.2/1.8/2.49/3.46	0.43/0.86/1.1/1.98/2.25	28.5/10/13.6/4.8/4.2	0.12×0.18
Ref. [12]	2.1/3.0/4.0/4.7/7.2	0.98/1.78/1.22/1.77/2.39	13.7/5.6/10.5/5.1/2.9	0.16×0.07
Ref. [13]	11.57/11.99/12.43/14.21/14.8	0.82/1.1/0.95/1.55/1.74	1.46/1.64/1.3/0.98/0.9	3.08×1.24
This work	**1.38/2.58/3.69/5.36/5.8**	**0.56/0.53/1.20/0.86/1.9**	**12.4/10.7/4.61/5.71/3.05**	0.29×0.34

4. CONCLUSIONS

Stub-loaded step-impedance resonator (SLSIR) is a simple resonator structure which has multi-resonant modes to be controlled by adjusting the structure parameters. In this paper, only two SLSIRs are used to achieve a quint-band responses. Resonant properties of the SLSIR are analyzed by using odd and even mode impedance analysis, clearly showing the frequency ratios of the high order modes to the fundamental mode of the SLSIR depending on the impedance ratio and length ratio of the SLSIR. Electric coupling and connectedwith 0° feeding input/output structure are used for the filter formation since the coupling coefficients and external quality factors can be calculated to determine the filter response. The designed filter has center frequencies at 1.38 GHz, 2.58 GHz, 3.69 GHz, 5.36 GHz, and 5.8 GHz, corresponding to the GPS, 4G, WiMAX, and WLAN applications. The filter is designed, fabricated, and measured. Measured results have an agreement with simulated ones and verify the design concept.

ACKNOWLEDGMENT

The authors acknowledge Mr. Hong-Zheng Lai and Dr. Shih-Kun Liu for the help with sample measurement.

REFERENCES

1. Luo, S., L. Zhu, and S. Sun, "Compact dual-mode triple-band bandpass filters using three pairs of degenerate modes in a ring resonator," *IEEE Trans. Microw. Theory Tech.*, Vol. 59, No. 5, 1222–1229, May 2011.
2. Chen, W. Y., S. J. Chang, M. H. Weng, Y. H. Su, and H. Kuan, "Simple method to design a tri-band bandpass filter using asymmetric SIRs for GSM, WiMAX and WLAN applications," *Microwave Opt. Tech. Lett.*, Vol. 53, No. 7, 1573–1576, Jul. 2011.
3. Chen, W. Y., M. H. Weng, and S. J. Chang, "A new tri-band bandpass filter based on stub-loaded stepped impedance resonator," *IEEE Microw. Wireless Compon. Lett.*, Vol. 22, 179–181, Apr. 2012.
4. Chen, C. F., T. Y. Huang, and R. B. Wu, "Design of dual- and triple-passband filters using alternately cascaded multiband resonators," *IEEE Trans. Microw. Theory Tech.*, Vol. 54, No. 9, 3550–3558, Sep. 2006.
5. Hsu, C. I. G., C. H. Lee, and Y. H. Hsieh, "Tri-band bandpass filter with sharp passband skirts designed using tri-section SIRs," *IEEE Microw. Wireless Compon. Lett.*, Vol. 18, No. 1, 19–21, Jan. 2008.
6. Chen, F. C. and Q. X. Chu, "Design of compact quad-band bandpass filters using assembled resonators," *Microwave Opt. Tech. Lett.*, Vol. 53, No. 6, 1305–1308, Jun. 2011.
7. Hsu, K. W., W. C. Hung, and W. H. Tu, "Compact quint-band microstrip bandpass filter using double-layered substrate," *IEEE MTT-S Int. Microw. Symp. Dig.*, Vol. 7, No. 6, 1041–1044, Jun. 2013.
8. Chen, C. F., "Design of a compact microstrip quint-band filter based on the tri-mode stub-loaded stepped- impedance resonators," *IEEE Microw. Wireless Compon. Lett.*, Vol. 22, No. 7, 357–359, Jul. 2012.
9. Chen, L. and F. Wei, "Compact quad-and quint-band BPFs based on multimode stub loaded resonators," *Microwave Opt. Tech. Lett.*, Vol. 57, No. 12, 2837–2841, Dec. 2015.
10. Xu, J., W. Wu, and G. Wei, "Compact multi-band bandpass filters with mixed electric and magnetic coupling using multiple-mode resonator," *IEEE Trans. Microw. Theory Tech.*, Vol. 63, No. 12, 3909–3920, Dec. 2015.
11. Zhu, C. M., J. Xu, W. Kang, and W. Wu, "Compact QB-BPF based on single PMR," *Electronics Lett.*, Vol. 52, No. 17, 1463–1465, 2016.
12. Ai, J., Y. Zhang, K. D. Xu, D. Li, and Y. Fan, "Miniaturized quint-band bandpass filter based on multi-mode resonator and $\lambda/4$ resonators with mixed electric and magnetic coupling," *IEEE Microw. Wireless Compon. Lett.*, Vol. 26, No. 5, 343–345, May 2016.
13. Zhou, K., C. X. Zhou, H. W. Xie, and W. Wu, "Synthesis design of SIW multiband bandpass filters based on dual-mode resonances and split-type dual- and triple-band responses," *IEEE Trans. Microw. Theory Tech.*, Vol. 67, No. 1, 151–161, Jan. 2019.
14. Hong, J. S., *Microstrip Filters for RF/Microwave Applications*, 2nd Edition, Wiley, New York (NY), 2011.
15. IE3D Simulator; Zeland Software, Inc. CA, USA, 2002.
16. Tsai, C. M., S. Y. Lee, and C. C. Tsai, "Performance of a planar filter using a 0° feed structure," *IEEE Trans. Microw. Theory Tech.*, Vol. 50, No. 10, 2362–2367, Nov. 2002.